Effects of large amounts of hydrogen on the fatigue crack growth behavior of torsional prestrained carbon steel

Yuta Matsuda
Advanced Engineering Course, National Institute of Technology, Sasebo College, Japan
me1419@st.sasebo.ac.jp

Hiroshi Nishiguchi, Takayuki Fukuda
Department of Mechanical Engineering, National Institute of Technology, Sasebo College, Japan
hiroshin@sasebo.ac.jp

ABSTRACT. The effects of large amounts of hydrogen on the fatigue crack growth properties of torsional prestrained ferritic–pearlitic low-carbon steel were investigated. Hydrogen-precharged specimens were produced by conducting cathodic charge to the virgin material and to torsional prestrained JIS-S10C and JIS-S25C steels (hereafter S10C and S25C steels). Rotating bending fatigue tests were conducted in air at room temperature. Hydrogen content, C_H, increased with torsional prestrain for both S10C and S25C steels; the C_H of the torsional prestrained S25C steel precharged with hydrogen was lower than that of S10C at the same torsional prestrain. No clear difference between the maximum C_H values of the torsional fractured S10C and S25C hydrogen-precharged steel specimens. With respect to crack initiation, there was no obvious difference between the uncharged and precharged specimens in spite of the large amount of C_H induced by torsional prestrain. The acceleration of fatigue crack growth by hydrogen was the main cause of the decreased fatigue life. For the virgin material, hydrogen had no obvious effect on the fatigue crack growth rate. In contrast, for the torsional prestrained materials, the acceleration ratios, $\{(da/dN)_H/(da/dN)_U\}$, increased with the torsional prestrain and C_H. However, $\{(da/dN)_H/(da/dN)_U\}$ did not exceed the value of about 30, even when a large amount of hydrogen was charged ($10.0 \leq C_H \leq 30.3$ mass ppm). A hydrogen content threshold was found; hydrogen content above this limit enhances the growth of the non-propagated crack, even for metals with lower hardness (HV < 200).

KEYWORDS. Fatigue crack growth property; Non-propagating crack; Torsional prestrain; Large amounts of hydrogen; Carbon steel.

INTRODUCTION

Recently, hydrogen energy systems have been proposed as an alternative energy source to solve environmental and energy problems related to the depletion of fossil fuel, global warming, and the nuclear reactor accident caused by the eastern Japan great earthquake of 2011. However, it has been reported that the strength properties of

materials that are directly exposed to high-pressure hydrogen gas are degraded. This problem is known as hydrogen embrittlement. The effects of hydrogen on fatigue crack growth properties within the low and middle stress intensity factor ranges have been investigated. [1, 2] The findings of these studies have provided important insights that can be used to inform the design of hydrogen-related devices for a future hydrogen economy. Hydrogen pre-charging was reported to increase the fatigue crack growth acceleration rate of 0.08 mass%C ferritic–pearlitic carbon steel JIS-SGP, compared with the uncharged specimen [1]. The effect of hydrogen on fatigue crack growth rate was related to the test frequency; however, the enhancement in rate acceleration due to hydrogen reached an approximately 10 times rate, which should be an upper bound on the acceleration of fatigue crack growth by hydrogen. Another study indicated that the upper bound of fatigue crack growth acceleration in JIS-SM490B under a high-pressure hydrogen gas atmosphere is 30 times for hydrogen gas pressures less than 45 MPa [2]. These upper bounds have been used to predict fatigue life for the design of hydrogen-related devices. In addition, hydrogen was reported to have little effect on the fatigue limits of lower-hardness materials (HV ≤ 200), such as carbon steel, whereas for materials with higher hardness (HV ≥ 200), hydrogen decreased the fatigue limit by 25 % [3]. Previous review articles on the effects of internal hydrogen on fatigue properties mainly discussed low hydrogen contents. However, the fatigue data for high hydrogen contents are important for the design of hydrogen-related devices. The effects of larger amounts of hydrogen on the crack growth rate and fatigue limit have not been studied because the hydrogen contents of BCC materials precharged with hydrogen are small. According to recent studies, hydrogen diffuses to and concentrates at fatigue crack tips. Therefore, it is important to clarify the effects of larger amounts of hydrogen during the design stage of a hydrogen-related device. According to a previous study by the authors using prestrained carbon steels, hydrogen content increases with the prestrain [4]. Furthermore, for torsional prestrained JIS-S25C steel (hereafter S25C steel) specimens, it is possible to introduce a larger amount of hydrogen into carbon steel (up to 35 mass ppm) than that into the tensile prestrained material. Therefore, in this study, the effects of large amounts of hydrogen on fatigue crack growth and fatigue limit were investigated using two carbon steels (JIS-S10C and JIS-S25C steels, hereafter S10C and S25C steels).

MATERIALS AND EXPERIMENTAL METHODS

The materials used in this study were ferritic–pearlitic carbon steels S10C and S25C. Tab. 1 shows the chemical compositions and Vickers hardness values (indentation force, 9.8 kN; holding time, 30 s; number of measured points, 20) of the steels. Heat treatment was conducted for 1 h at 920 °C (S10C steel) or 900 °C (S25C steel). The Vickers hardness was HV = 97.8 for S10C steel and HV = 129 for S25C steel. Fig. 1 shows the shapes and dimensions of the rotating bending fatigue test and hydrogen measurement test specimens. Fig. 2 shows the results of torsional prestrain testing. After polishing with #2000 emery paper, all specimen surfaces were finished by buffing. The specimens were then subjected to torsional prestrain testing to yield torsional prestrained specimens. The specific angles of twist (θ_{pre}) ranged from 0 to 45.0 deg/mm for S10C steel and from 0 to 20.0 deg/mm for S25C steel. After testing, the prestrained specimens were finished by rebuffing, and small holes with diameters of 500 μm and depths of 500 μm were introduced into the rotating bending fatigue test specimens.

C	Si	Mn	P	S	HV
0.10	0.17	0.36	0.09	0.17	97.8

(a) S10C steel

C	Si	Mn	P	S	HV
0.22	0.20	0.39	0.010	0.018	125

(b) S25C steel

Table 1: Chemical compositions (mass %) and Vickers hardness values of the experimental steels.

Rotating bending fatigue tests were conducted at room temperature in air. Cracks were observed using the replica method, and the crack lengths ($2a$) were measured. Hydrogen was charged into the virgin and torsional prestrained specimens of S10C and S25C steels using the cathodic charge method with a platinum electrode at a current density of 100 A/m^2 in an aqueous solution of H_2SO_4 (pH 2.0) at 313 K for 24 h. Hydrogen content was previously confirmed to be saturated in

each specimen. Hydrogen content was measured using gas chromatography thermal desorption analysis (TDA). The rate of temperature increase was 0.028 °C/s. During hydrogen charging, the areas of fatigue cracking and small artificial holes were locally protected to prevent corrosion. After removing the protection, rotating bending fatigue tests were conducted for both specimens (S10C and S25C steels) at test frequencies of f = 1.6–3.2 Hz, corresponding to stress amplitudes of σ_a = 250 MPa. The fatigue tests at fatigue limit were conducted at f = 30 Hz and σ_a = 150 MPa for S10C torsional prestrained (θ_{pre} = 45.0 deg/mm) steel and at f = 30 Hz and σ_a = 135 MPa for S25C torsional prestrained (θ_{pre} = 20.0 deg/mm) steel. The stress intensity factor was calculated according to the handbook [5].

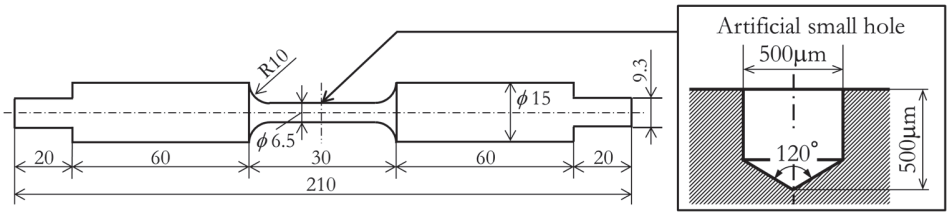

(a) Rotating bending fatigue test specimen

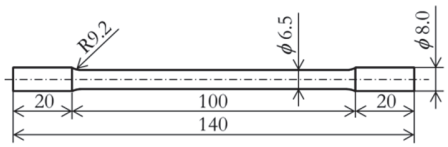

(b) Hydrogen measurement specimen

Figure 1: The shapes and dimensions of specimens (mm).

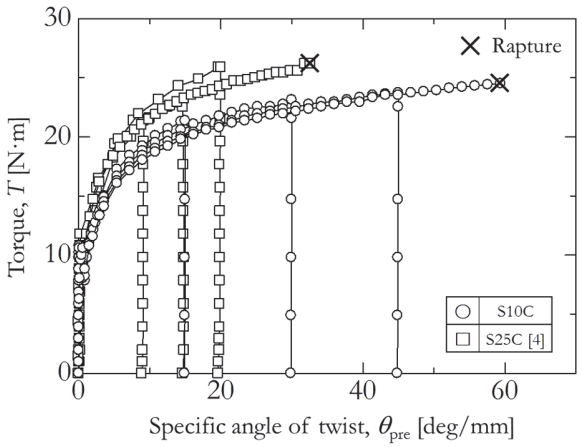

Figure 2: Relationship between torque and specific angle of twist.

RESULTS AND DISCUSSION

Effect of torsional prestrain on hydrogen entry properties

Fig. 3 shows the TDA hydrogen release profiles during continuous heating of hydrogen-precharged S10C and S25C specimens. As shown in Fig. 3(a), the hydrogen desorption peaks were located at around 100–150 °C for virgin and prestrained specimens for both S10C and S25C steels. The height of the peak increases with the prestrain due to the increasing density of dislocations, which act as hydrogen trap sites. Hydrogen released from around 20–200 °C is classified as diffusible hydrogen and causes hydrogen embrittlement because hydrogen can diffuse to crack tips or regions of stress concentration [6]. Small peaks corresponding to the so-called non-diffusible hydrogen were observed at temperatures close to 300 °C.

Fig. 4 shows the relation between hydrogen content (C_H) and equivalent prestrain at the specimen surface ($\varepsilon_{eq,s}$) along with the specific angle of twist (θ_{pre}). Previous results [4] for S25C steel are also included in Fig. 4. Hydrogen content increased with the prestrain. Compared with that of S25C steel, C_H of S10C steel is smaller at the same torsional prestrain due to the difference in the fraction of pearlite. As shown in Fig. 4, S10C steel has a higher ductility than S25C steel; thus, higher prestrain can be introduced into S10C steel. However, no clear difference in the maximum hydrogen contents in torsional fracture specimens between S10C and S25C steels exists. In S25C steel, for $\theta_{pre} \geq 25.0$ deg/mm, some cracks are initiated during the introduction of torsional prestrain. In contrast, for the prestrained S10C steel specimen, few cracks are initiated, even when $\theta_{pre} = 45.0$ deg/mm. Therefore, a fatigue test with a hydrogen-precharged specimen containing a large hydrogen content ($C_H = 36.7$ mass ppm) could be conducted using torsional prestrained ($\theta_{pre} = 45.0$ deg/mm) S10C steel.

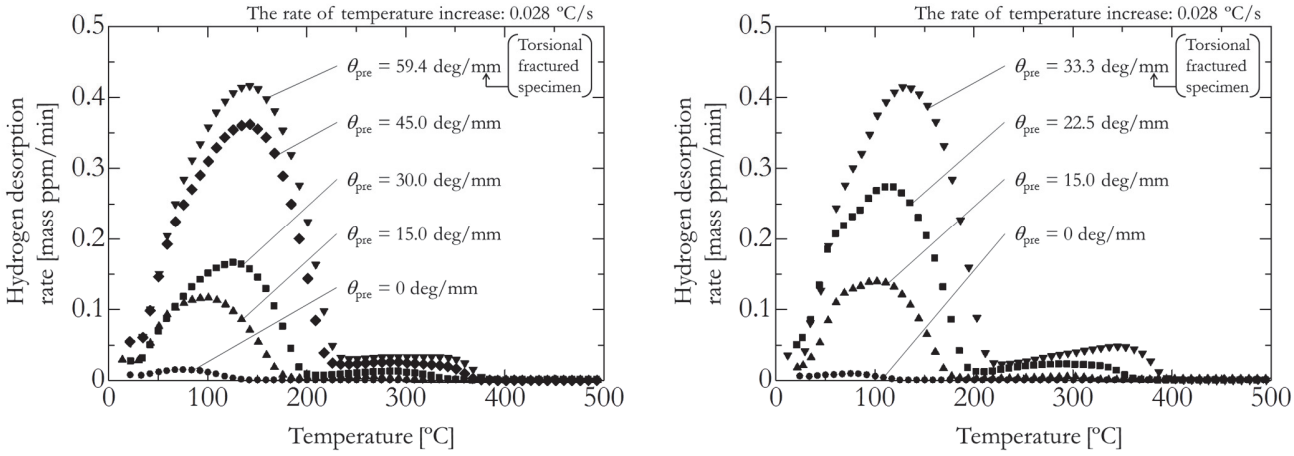

(a) S10C steel (b) S25C steel [4]

Figure 3: TDA hydrogen release profiles during continuous heating of hydrogen-precharged S10C and S25C specimens. θ_{pre}: Specific angle of twist.

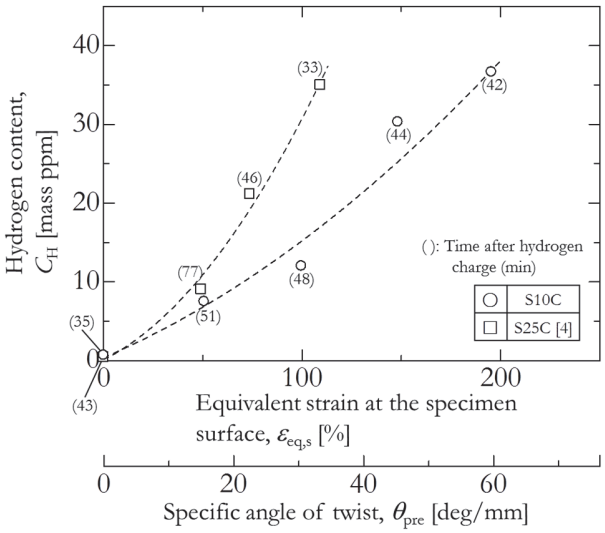

Figure 4: Relationship between hydrogen content and $\varepsilon_{eq,s}$.

Effects of a large amount of hydrogen on the fatigue property of carbon steel

Fig. 5 shows the relations between the number of cycles to failure (N_f) and equivalent strain at the specimen surface ($\varepsilon_{eq,s}$). The uncharged virgin specimen fractured after 3.67×10^4 cycles, whereas the fatigue lives of both S10C and S25C steels increased with the torsional prestrain due to work hardening. However, in specimens precharged with hydrogen, fatigue life decreased with increasing prestrain. Fig. 6 shows the relations between crack length ($2a$) and number of cycles (N) for S10C and S25C steels. With respect to crack initiation, there is no obvious difference between the uncharged and

hydrogen-precharged specimens in spite of the large amount of hydrogen introduced by torsional prestrain. For the virgin specimen, hydrogen does not affect crack growth or initiation. However, for all torsional prestrained specimens, the presence of hydrogen accelerated crack growth; thus, the N_f values of torsional prestrained specimens precharged with hydrogen were clearly decreased.

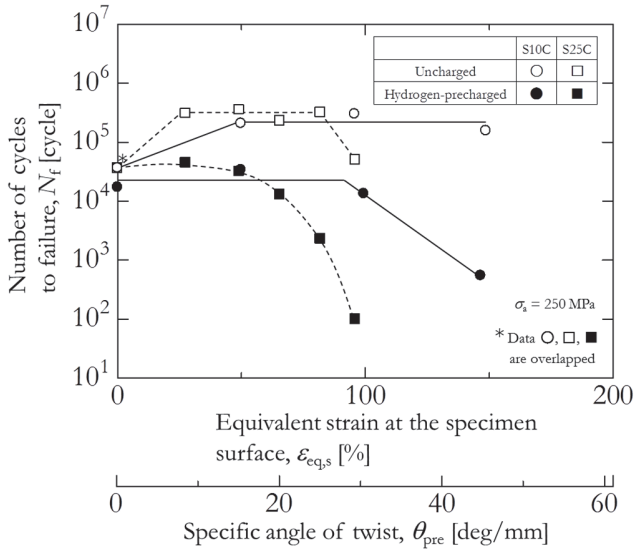

Figure 5: Relations between number of cycles to failure and $\varepsilon_{eq,s}$.

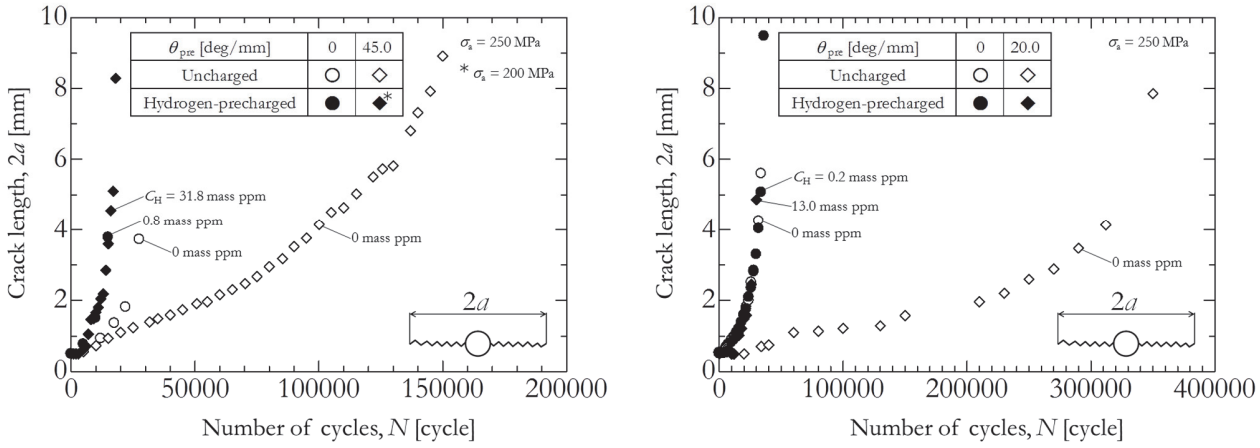

(a) S10C steel (b) S25C steel

Figure 6: Relations between crack length and number of cycles. θ_{pre}: Specific angle of twist.

Effects of a large amount of hydrogen on the fatigue crack growth acceleration rate of carbon steel

Fig. 7 shows the relation between fatigue crack growth rate (da/dN) and stress intensity factor range (ΔK) for S10C steel. For the virgin material, no obvious effect of hydrogen on the fatigue crack growth rate was observed. For torsional prestrained materials, the acceleration ratios $\{(da/dN)_H/(da/dN)_U\}$ were estimated, where $(da/dN)_H$ represents the value of da/dN for the hydrogen-precharged specimen, and $(da/dN)_U$ is the da/dN for the uncharged specimen. For instance, when θ_{pre} = 15.0 deg/mm, $\{(da/dN)_H/(da/dN)_U\}$ = 4 at ΔK = 15 MPa$\sqrt{m}$, indicating that the fatigue crack growth rate of the hydrogen-precharged specimen is 4 times higher than that of the uncharged specimen. For θ_{pre} = 30.0 deg/mm, $\{(da/dN)_H/(da/dN)_U\}$ = 13 at ΔK = 15 MPa$\sqrt{m}$. These results show that the fatigue crack growth rate of hydrogen-precharged materials increases with the hydrogen content (C_H). For θ_{pre} = 45.0 deg/mm the results were drown by dot lines at positions apart far from other prestrained specimens. $\{(da/dN)_H/(da/dN)_U\}$ for θ_{pre} = 45.0 deg/mm was about 16 at ΔK = 15 MPa$\sqrt{m}$, which is almost the same as that obtained for θ_{pre} = 30.0 deg/mm. Fig. 8 shows the relation

between fatigue crack growth rate (da/dN) and stress intensity factor range (ΔK) for S25C steel. S25C steel exhibits similar tendencies in the acceleration and saturation of fatigue crack growth rate in the θ_{pre} range of 0–20.0 deg/mm.

Based on these results, Fig. 9 shows the relation between $\{(da/dN)_H/(da/dN)_U\}$ and C_H. The fatigue crack growth acceleration rates of S10C and S25C steels do not increase, even when C_H exceeds 10 mass ppm. This indicates that $\{(da/dN)_H/(da/dN)_U\}$ has an upper bound estimated to be in the range of about 30 for both S10C and S25C steels.

At this point, the effects of hydrogen precharging on fatigue crack growth rate have been reported in the previous studies. In case of 0.08 mass%C ferritic–pearlitic carbon steel (C_H = 1.0 mass ppm), for $f \leq 0.01$ Hz, the fatigue crack growth acceleration rate $\{(da/dN)_H/(da/dN)_U\}$ = 10 [1]. Tanaka et al. [7] reported a $\{(da/dN)_H/(da/dN)_U\}$ upper bound of 30 for Cr–Mo steel, JIS-SCM435, (HV = 330; C_H = 0.24–0.59 mass ppm). Previous studies indicate that the maximum upper bound of $\{(da/dN)_H/(da/dN)_U\}$ is about 30 for small hydrogen contents. In this study, even for large hydrogen contents, the maximum upper bound remained at around 30.

The upper bound value found in this study can be used as one parameter in the design of hydrogen-related devices. Further investigation is important to consider $\{(da/dN)_H/(da/dN)_U\}$ at lower frequencies.

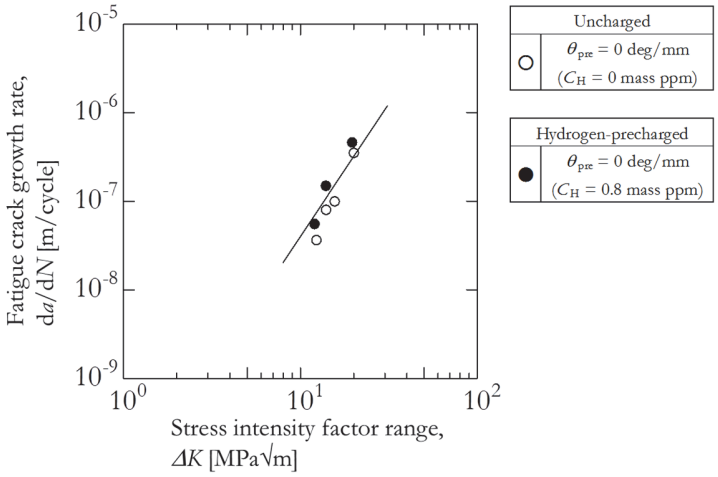

(a) Virgin materials

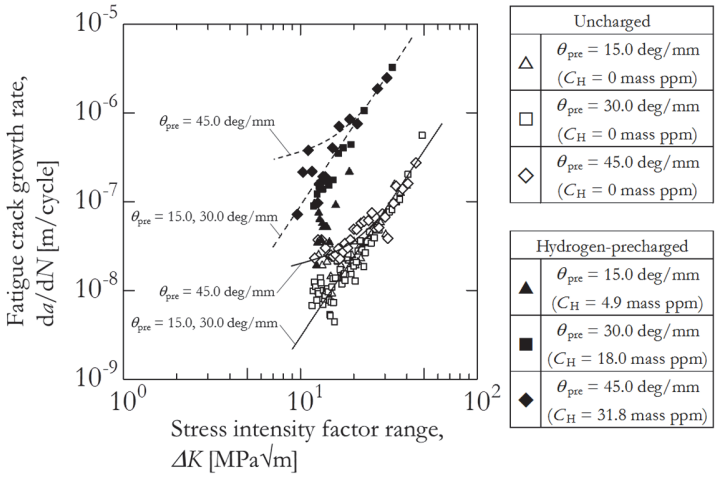

(b) Torsional prestrained materials

* The dotted line shows 30 times acceleration of fatigue crack growth rate for hydrogen-precharged specimen than the uncharged specimen.

Figure 7: Relations between fatigue crack growth rate and stress intensity factor range in S10C steel. θ_{pre}: Specific angle of twist.

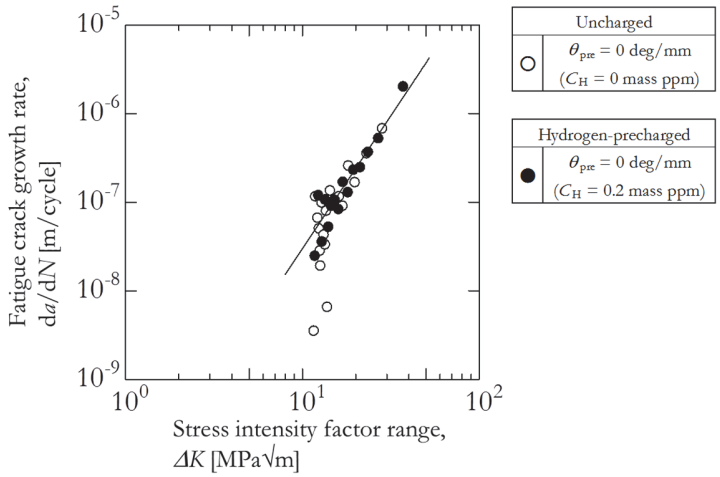

(a) Virgin materials

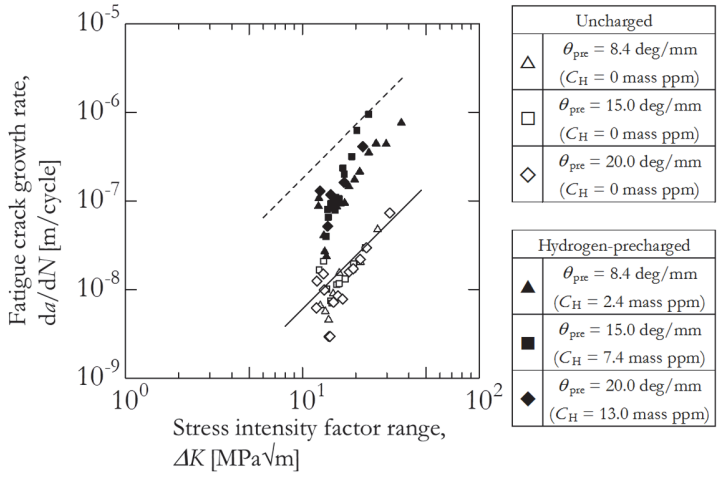

(b) Torsional prestrained materials

* The dotted line shows 30 times acceleration of fatigue crack growth rate for hydrogen-precharged specimen than the uncharged specimen.

Figure 8: Relations between fatigue crack growth rate and stress intensity factor range in S25C steel. θ_{pre}: Specific angle of twist.

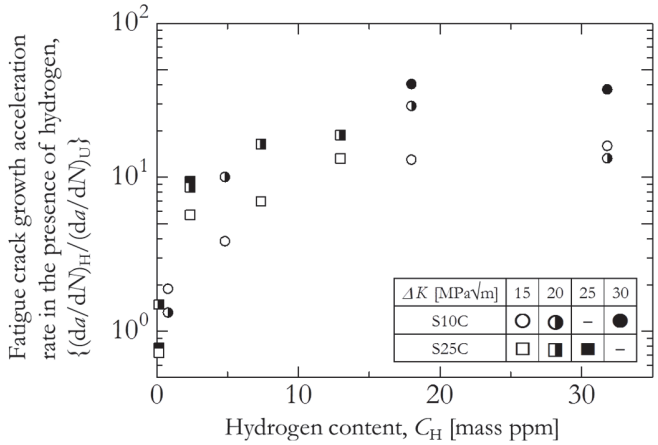

Figure 9: Relation between fatigue crack growth acceleration rate in the presence of hydrogen and hydrogen content. θ_{pre}: Specific angle of twist.

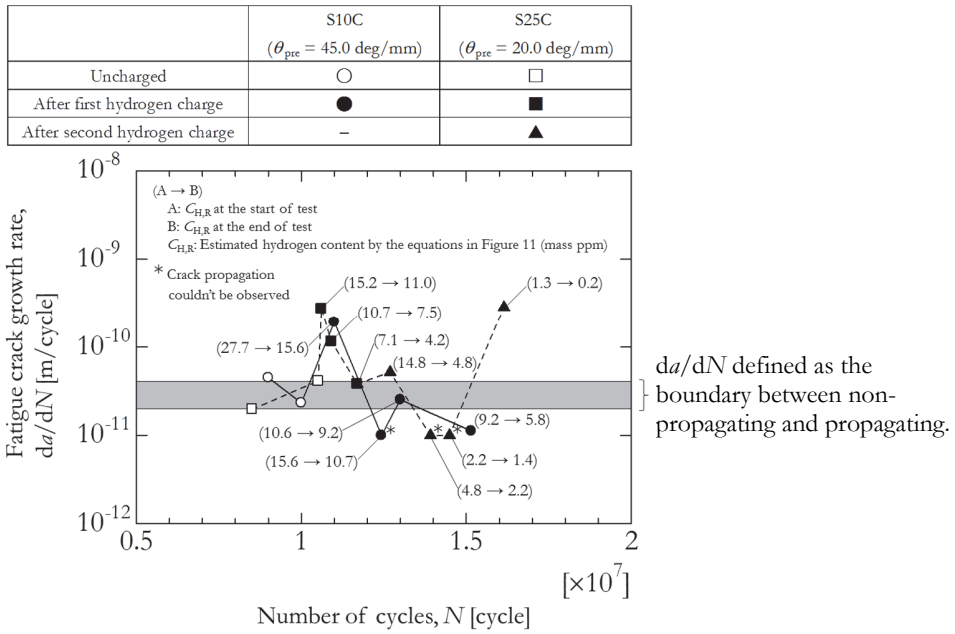

Figure 10: Relation between fatigue crack growth rate and number of cycles (f = 30 Hz). θ_{pre}: Specific angle of twist.

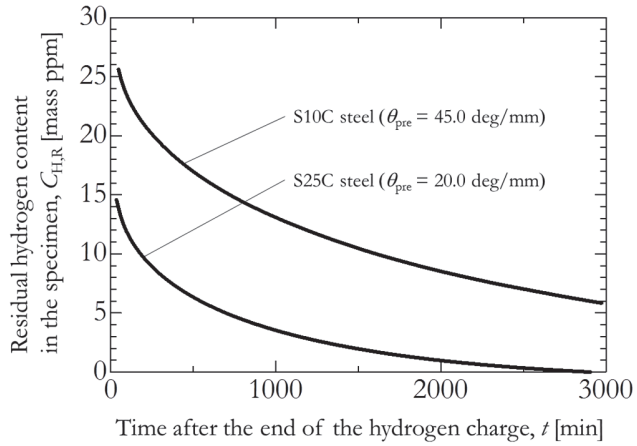

Figure 11: Relation between residual hydrogen content in the specimen and time after the end of hydrogen charge for the torsional prestrained S10C and S25C steel. θ_{pre}: Specific angle of twist.

Effects of a large amount of hydrogen on the fatigue limit of carbon steel

Fig. 10 shows the relation between da/dN and N, while Fig. 11 shows the relation between the residual hydrogen content (diffusible hydrogen content) in the specimen and time, following the first hydrogen charging of the torsional prestrained (θ_{pre} = 45.0 deg/mm) S10C steel and (θ_{pre} = 20.0 deg/mm) S25C steel. The results shown in Fig. 11 were obtained by measuring the hydrogen content of the hydrogen measurement specimen (Fig. 1(b)) used for TDA at 30 °C and heated to 520 °C after 48 h. The hydrogen content values during the fatigue test shown in Fig. 10 were calculated using the results given in Fig. 11. The fatigue test of the torsional prestrained (θ_{pre} = 20.0 deg/mm) uncharged S25C specimen was first conducted at σ_a = 135 MPa. Under this condition, a non-propagating crack was observed at the edge of the artificial small hole, and the fatigue crack growth rates were da/dN = 2.0 × 10^{-11} m/cycle at N = 8–9 × 10^6 cycles and da/dN = 4.1 × 10^{-11} m/cycle at N = 9–10 × 10^6 cycles. Hence, da/dN = 2.0 × 10^{-11} to 4.1 × 10^{-11} m/cycle was defined as the threshold da/dN value between non-propagation and propagation in this paper. After hydrogen charging, the observed da/dN was greater than 10^{-10} m/cycle, indicating crack propagation. Following this propagation, da/dN then decreased to 3.8 × 10^{-11} m/cycle, while the estimated hydrogen content decreased to 7.1–4.2 mass ppm. Then, the same specimen was hydrogen

charged for a second time with almost the same amount of hydrogen as in the first charging, as was previously confirmed. At the beginning of the repeat fatigue test, da/dN was 5.2 × 10^{-11} m/cycle, which is slightly higher than the 4.1 × 10^{-11} m/cycle threshold value, indicating crack propagation. However da/dN then decreased to 1.0 × 10^{-11} m/cycle and crack propagation was not clearly observed; this was accompanied by a decrease in hydrogen content to less than 4.8 mass ppm. Hence, it was presumed that hydrogen enhances the growth of a non-propagating crack.

However, in the case involving hydrogen content of less than 4.8 mass ppm, the non-propagating crack was not caused to propagate by the hydrogen. The explanation for this behavior is that, as the hydrogen was released into the atmosphere during the test, there was insufficient contained hydrogen for enhancement of the fatigue crack growth. At the end of the S25C steel fatigue test, crack propagation occurred at a lower hydrogen content. It is possible that small cracks initiated by the introduction of the torsional prestrain grew in locations other than the main crack site, and all of these cracks then coalesced. For a hydrogen content range of 4.8 to 1.4, the main crack did not propagate at the surface, however it was presumed that the small cracks propagated and coalesced with the main crack at a subsurface. Then, the main crack finally exhibited propagation at a lower hydrogen content, due to coalescence between the small cracks and the main crack. Thus, in the case involving hydrogen content of less than 4.8 mass ppm, the hydrogen itself did not enhance the main crack growth.

A similar fatigue test of torsional prestrained (θ_{pre} = 45.0 deg/mm) S10C steel was conducted at σ_a = 150 MPa. A non-propagating crack also occurred at the edge of the artificial small hole in the absence of hydrogen. The fatigue crack growth rates were da/dN = 4.5 × 10^{-11} m/cycle at N = 8–9 × 10^6 cycles and da/dN = 2.3 × 10^{-11} m/cycle at N = 9–10 × 10^6 cycles, which is almost identical to the defined da/dN threshold for a non-propagating crack for S25C steel. In the S10C steel case, secondary hydrogen charging was not conducted, because the hydrogen content was high (5.8 mass ppm), even after 5 × 10^6 cycles of the fatigue test.

At the beginning of the fatigue test of the hydrogen-charged S10C specimen, da/dN was greater than 10^{-10} m/cycle, indicating crack propagation. Fig. 10 shows that da/dN was decreased by increases in both time and N, while Fig. 12 shows photographs of the crack for N = 1.10 × 10^7 and 1.24 × 10^7 cycles after hydrogen charging of the S10C steel. Crack propagation was only clearly observed in this specimen. In the S10C prestrained specimen case, the hydrogen content was higher than that of the S25C prestrained specimen. However, crack propagation was arrested at a hydrogen content value of 15.6 to 10.7 mass ppm. Hence, 15.6 mass ppm hydrogen is the threshold value beyond which hydrogen enhances the propagation of an arrested crack. It has been reported that the fatigue limit of carbon steel with HV ≤ 200 is not reduced by hydrogen (S25C steel; HV = 129; C_H = 0.31 mass ppm) [3]. However, in the presence of higher hydrogen content, it is possible for hydrogen to enhance the propagation of an arrested crack even for these metals, as large amounts of hydrogen decrease the fatigue limit.

It seems that the difference in the hydrogen content threshold values for S10C (15.6 mass ppm) and S25C (4.8 mass ppm) steels is due to the densities of the small cracks initiated during the torsional prestraining. Because the pearlite content of S25C steel is greater than that of S10C, a greater number of pearlite cracks were initiated for S25C steel than for S10C.

This problem requires more investigation, in order to clarify the effects of the small cracks initiated during torsional prestraining on the non-propagating crack.

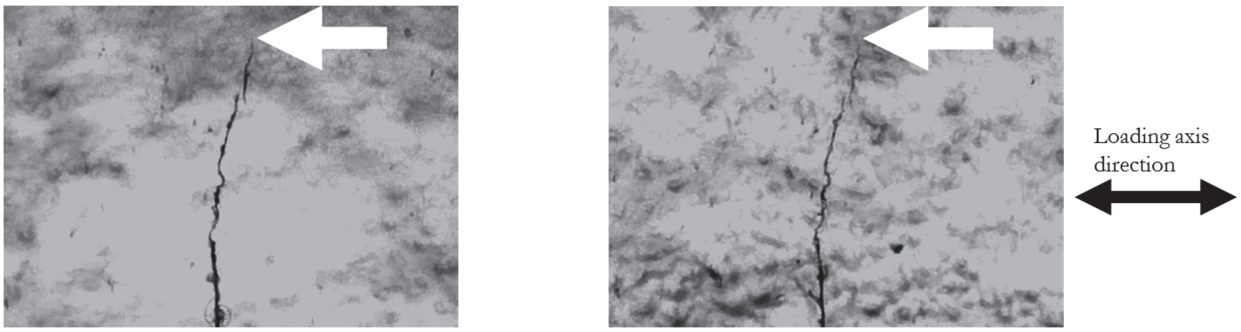

(a) N = 1.10 × 10^7 ($C_{H,R}$ = 15.6 mass ppm) (b) N = 1.24 × 10^7 ($C_{H,R}$ = 10.7 mass ppm)

Figure 12: Non-propagating crack (S10C; θ_{pre} = 45.0 deg/mm; σ_a = 150 MPa; f = 30 Hz). θ_{pre}: Specific angle of twist. $C_{H,R}$: Hydrogen content by the equations in Fig. 11.

CONCLUSIONS

The effects of hydrogen on the fatigue crack growth rates of torsional prestrained ferritic–pearlitic low-carbon steels (JIS-S10C and JIS-S25C steels) were investigated. The following conclusions were obtained.

1. Hydrogen content increased with the torsional prestrain for both S10C and S25C steels. The hydrogen content of hydrogen-precharged torsional prestrained S10C steel was lower than that of S25C steel at the same torsional prestrain. No clear difference in the maximum hydrogen contents between the hydrogen-precharged torsional fractured specimens of S10C and S25C steels existed.
2. With respect to crack initiation, there was no obvious difference between the uncharged and hydrogen-precharged specimens in spite of the large amount of C_H induced by torsional prestrain. The acceleration of fatigue crack growth by hydrogen was the main cause of the decreased fatigue life.
3. For the virgin material, no obvious effect of hydrogen on the fatigue crack growth rate was observed. In contrast, for torsional prestrained materials, the acceleration ratios, $\{(da/dN)_H/(da/dN)_U\}$, increased with the torsional prestrain and hydrogen content. However, an upper bound of $\{(da/dN)_H/(da/dN)_U\}$ of approximately 30 was observed, even when large amounts of hydrogen were charged ($10.0 \leq C_H \leq 30.3$ mass ppm).
4. A hydrogen content threshold was found; hydrogen content above this limit enhances the growth of the non-propagated crack, even for metals with lower hardness (HV < 200).

ACKNOWLEDGMENTS

This research has been supported by the NEDO project "Fundamental Research Project on Advanced Hydrogen Science (2006e2012)".

REFERENCES

[1] Saburo, M., Noriko, T., Yukitaka, M., Effects of Hydrogen on Fatigue Crack Growth and Stretch Zone of 0.08 mass%C Low Carbon Steel Pipe, Trans. Jpn. Soc. Mech. Eng. A, 74 (2008) 1528–1537.

[2] Michio, Y., Takashi, M., Noriko, T., Hisao, M., Saburo, M., Effects of hydrogen gas pressure and test frequency on fatigue crack growth properties of low carbon steel in 0.1–90 MPa, Trans. Jpn. Soc. Mech. Eng. A, 80 (2014) SMM0254–SMM0254.

[3] Yoshiyuki, K., Masanobu, K., Keiko, S., Jun-ichiro, Y., Effect of Absorbed Hydrogen on the Near Threshold Fatigue Crack Growth Behavior of Short Crack: Examination on Low Alloy Steel, Carbon Steel and Heat Resistant Alloy A286, Trans. Jpn. Soc. Mech. Eng. A, 74 (2008) 1366–1372.

[4] Hiroshi, N., Ryota, K., Takayuki, F., Effects of Hydrogen on Tensile and Torsional Strength Properties of Torsional Prestrained Ferritic-Pearlitic Carbon Steel, Proceedings of International Hydrogen Conference (IHC 2012).

[5] Yukitaka, M., Stress Intensity Factors Handbook (In 2 Volumes), Committee on Fracture Mechanics, Pergamon Press, Japan, (1987) 659–662.

[6] Takai, K., Watanuki, R., Hydrogen in Trapping States Innocuous to Environmental Degradation of High-strength Steels, ISIJ international, 43 (2003) 520–526.

[7] Tanaka, H., Homma, N., Matsuoka, S., Murakami, Y., Effect of Hydrogen and Frequency on Fatigue Behavior of SCM435 Steel for Storage Cylinder of Hydrogen Station (<Special Issue> Strength Problems of Materials Used for Hydrogen Energy System), Trans. Jpn. Soc. Mech. Eng. A, 73 (2007) 1358–1365.